Leptons: e, μ, τ + systematic uncertainties

Timothée Theveneaux-Pelzer[1], *Javier Fernandez Menendez*[2] on behalf of the ATLAS, CDF, CMS and D0 Collaborations

[1]Laboratoire de Physique Corpusculaire (LPC), Clermont Université, Université Blaise Pascal, CNRS/IN2P3, Clermont-Ferrand, France
[2]Universidad de Oviedo, Oviedo, Spain

DOI: http://dx.doi.org/10.3204/DESY-PROC-2014-02/3

An overview of the charged lepton performance in the ATLAS and CMS experiments at the LHC and in the CDF and D0 experiments at the Tevatron is given, in the specific context of physics analyses requiring the selection of leptons from top-quark decays. The trigger and reconstruction algorithms are presented, as well as the identification and isolation criteria, pointing out the specificities of top-quark analysis selections. The impact of the lepton-related experimental systematic uncertainties are discussed.

1 Introduction

The top quark decays mostly into a W boson and a b quark, and in roughly one third of the cases, the W decays into a neutrino and a charged lepton. Hence, the reconstruction of electrons, muons and taus plays a key role in the ability of the top-quark factories to select collision data samples enriched in top-quark events. The four general purpose hadron collider experiments - CDF [1] and D0 [2] at the Tevatron, ATLAS [3] and CMS [4] at the LHC - have developed similar strategies to select these prompt leptons produced in top-quark decays.

For prompt electron or muon triggering, reconstruction and identification, the experiments take advantage of the structure of the detectors, which include a tracker, calorimeters and muon spectrometers. Unlike leptonic taus - which are not distinguished from prompt electrons and muons in the reconstruction - the hadronic taus are also reconstructed, thanks to dedicated algorithms.

The experimental systematic uncertainties related to leptons arise mainly from the efficiency measurements which are necessary for modelling the detector acceptance, the lepton energy scale and resolution, and from the estimation of misidentified lepton background yields.

2 Trigger

The trigger systems of the four experiments share common features: they are divided in an hardware-based first level (L1) using coarse information, and in one or two software-based high level trigger (HLT) levels, which perform a finer reconstruction using the full granularity of the detectors. Top-quark analyses in the four experiments rely mainly on single-lepton trigger menus, with transverse energy (E_T) thresholds sufficient to cope with the high luminosity. Due to higher event rates, the thresholds are higher at the LHC, typically 24 GeV compared to

18 GeV at the Tevatron, for unprescaled triggers. However, in some cases multi-object triggers such as di-lepton or lepton plus jets are used, in order to increase the sensitivity.

2.1 Electrons

Electron trigger menus are seeded by L1 energy deposits in electromagnetic calorimeters above certain energy thresholds. In order to keep sustainable rates, requirements on the energy deposits in hadronic calorimeters can be applied to reject hadronic backgrounds. Then, the HLT algorithms perform a full reconstruction and apply identification and isolation criteria similar to those used offline. Figure 1 show the trigger efficiency as a function of the offline reconstructed electron transverse energy in ATLAS and CMS. The typical plateau efficiency is 95% for the identification criteria used in top-quark related analyses.

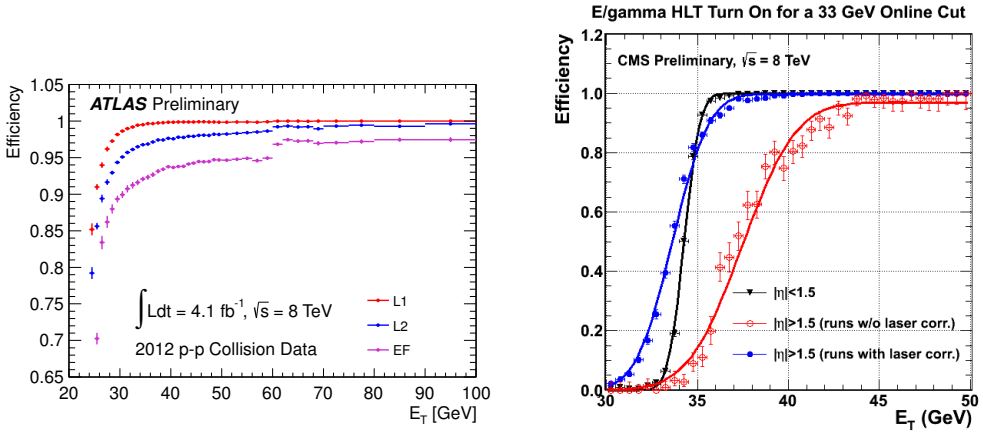

Figure 1: Trigger efficiency for a single electron menu with a 24 GeV threshold in ATLAS [5] (left) and with a 33 GeV threshold in CMS [6] (right).

2.2 Muons

The muon L1 trigger is mostly based on the muon spectrometer system, using fast muon chambers dedicated to the trigger. The HLT performs a full reconstruction combining both the muon chambers and the inner tracker, applying several quality cuts. Figure 2 shows the trigger efficiency with respect to the reconstructed muon transverse momentum in ATLAS and CMS. The typical plateau efficiency values span from 93 % to 98%, depending on the required quality criteria.

2.3 Taus

The tau trigger menus rely on calorimeter deposits with isolation criteria at L1, refined with several additional criteria to reject jet backgrounds at HLT using either the isolation, the track multiplicity or the shower shapes, similarly to the offline identification procedures later described. At LHC, the tau trigger energy thresholds span between 20 and above 100 GeV at

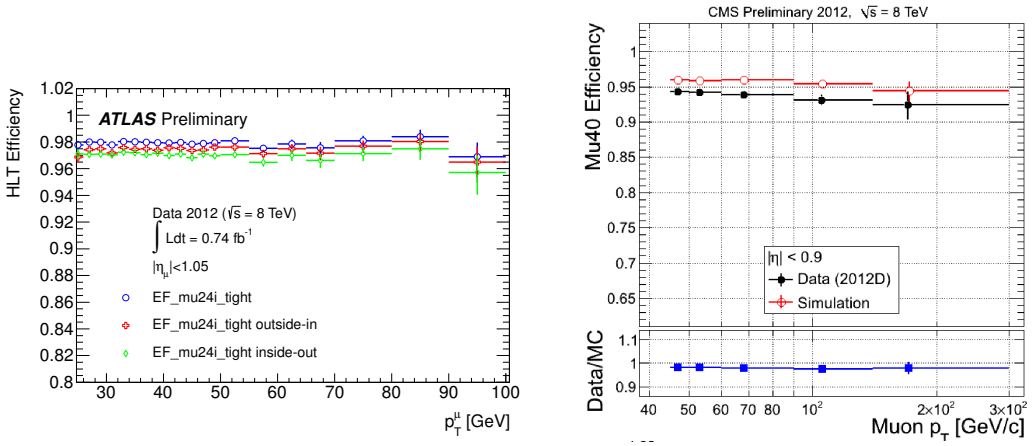

Figure 2: Trigger efficiency for a single muon menu with a 24 GeV threshold in ATLAS [7] (left) and with a 40 GeV threshold in CMS [6] (right).

HLT for the 2012 run. Figure 3 shows the trigger efficiency versus the tau candidate transverse momentum, for a 20 GeV single tau trigger chain in ATLAS. Its plateau efficiency is of the order of 80 %. The advantage of using dedicated tau triggers in D0 is also illustrated in Figure 3, in which the efficiency curve for single-jet and single-tau menus is compared.

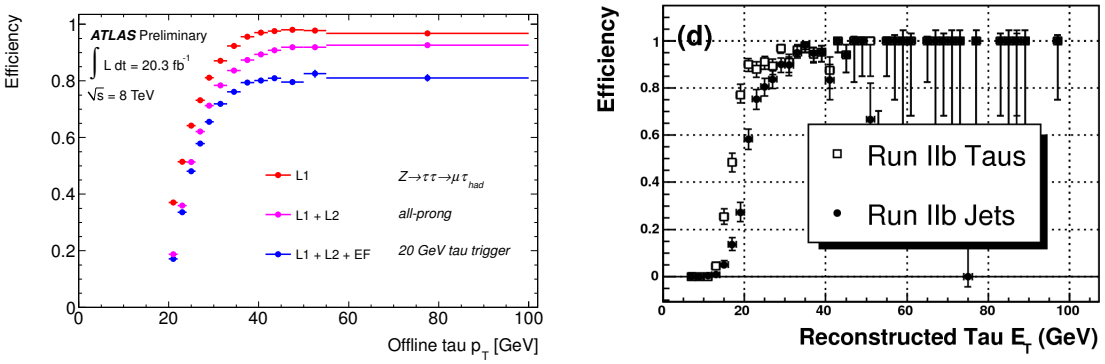

Figure 3: Trigger efficiency as a function of the transverse momentum for a single hadronic tau chain with a threshold of 20 GeV in ATLAS [8], measured on data using $Z \to \tau\tau$ events (left). Trigger efficiency as a function of the reconstructed tau transverse energy for a single hadronic tau L1 menu with a threshold of 15 GeV compared with a single jet L1 menu with a threshold of 20 GeV in D0 [9], measured on data using $Z \to \tau\tau$ events (right).

3 Reconstruction and identification

3.1 Electrons

Both the inner trackers and the electromagnetic calorimeters are used to perform offline electron reconstruction. Electron objects are reconstructed by the angular association of an electromagnetic calorimeter cluster and a charged track. The use of tracking algorithms which take into account the bremsstrahlung radiation energy losses allows to improve this association, and hence the reconstruction efficiency. Figure 4 shows the electron reconstruction efficiency in ATLAS as a function of the electron transverse energy, with (in 2012) and without (in 2011) using this improved tracking. The typical efficiency is about 98 % above 30 GeV, in both CMS (not shown) and ATLAS.

Identification criteria are further applied to reject experimental backgrounds, such as hadrons and converted photons. They make use of calorimeter shower shapes, energy leakage in the hadronic calorimeter, and track quality, and can be combined using multivariate techniques such as in CMS, or using E_T- and η-dependent rectangular cuts such as in ATLAS for top-quark analyses. Categories are defined depending on the strictness of the criteria, with different efficiency and background rejection factors. Figure 4 shows the identification efficiency in CMS as a function of the electron transverse energy in the pseudo-rapidity range $0 < |\eta| < 0.8$, for a category optimised to give an efficiency greater than 85 % in this central region.

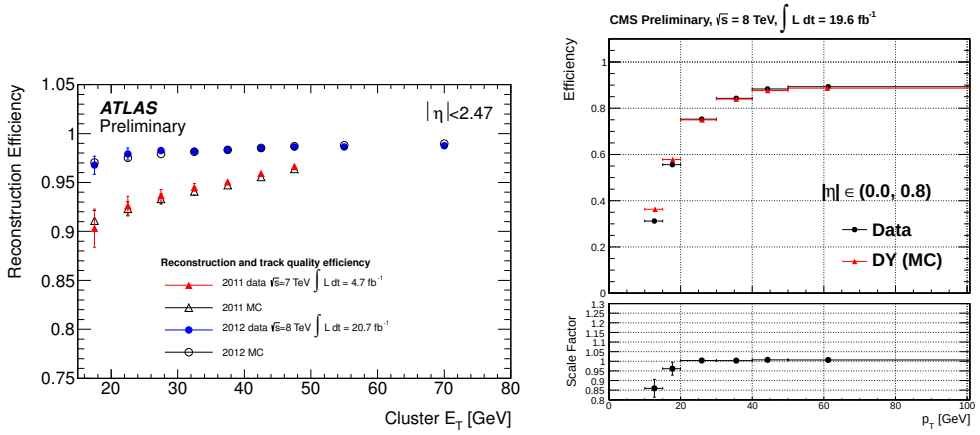

Figure 4: Electron reconstruction efficiency in ATLAS as a function of the transverse energy [10] (left) measured on 2011 and 2012 data. Electron identification efficiency as a function of the transverse momentum in CMS, for a typical identification category [11] (right).

In addition to the identification requirements described above, isolation cuts are applied in order to reject the non-prompt leptons from heavy flavour jets and to reduce the sensitivity to pile-up. For top-quark analyses, CMS uses particle-based relative isolation while ATLAS considers calorimeter and tracker absolute isolation, both in fixed-size cones.

3.2 Muons

Muons may be reconstructed with track fitting algorithms separately by muons chambers and from the inner tracker. Depending on the used sub-detectors, the reconstructed objects are divided in different categories. In most top-quark analyses, the selected muons are reconstructed by combining both systems. Additional requirements may be applied, such as track quality cuts in order to reject punch-through, criteria on angular or timing properties to remove cosmic muons in di-muon events, or on the quality of the trajectory fit to cope with hadron in-flight decays. Figure 5 shows the reconstruction efficiency for muons using both the tracker and the muon chambers as a function of the transverse momentum in ATLAS, and the identification criteria for reconstructed muons using the tightest reconstruction and identification criteria as a function of the pseudo-rapidity in CMS. The combined efficiency after application of such requirements is typically better than 95 %.

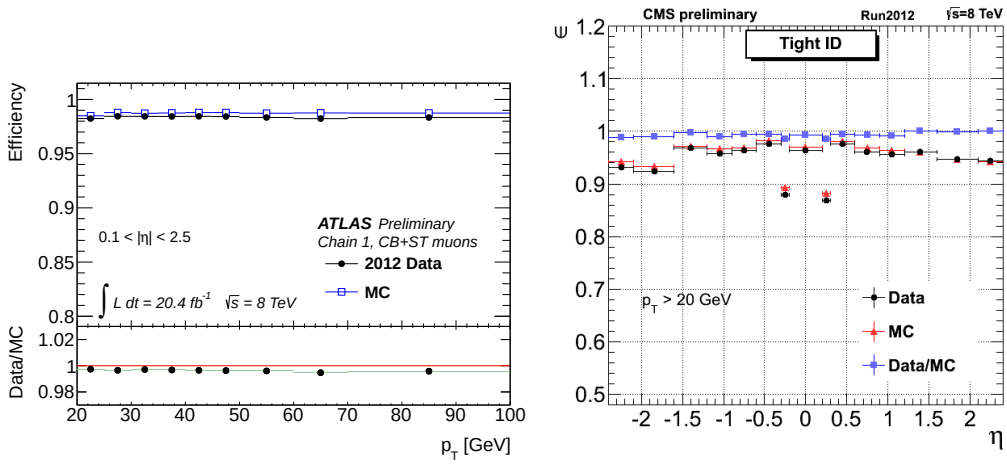

Figure 5: Muon reconstruction efficiency in ATLAS [12] (left) as a function of the transverse momentum, and muon identification efficiency as a function of the pseudo-rapidity in CMS [13] (right), for two typical object categories.

As for the electron case, isolation cuts are applied in order to improve the purity. The use of relative isolation with a decreasing cone size for increasing muon transverse momenta allows to cope with efficiency losses in boosted topologies in ATLAS.

3.3 Taus

The decay products of two thirds of the hadronically decaying taus consist predominantly of one or three charged pions, in addition to a neutrino and possibly neutral pions. The reconstruction and the identification of these hadronic taus rely on topological properties of calorimeter deposits. In ATLAS, jets with one or three associated tracks are selected, while CMS uses particle flow techniques to reconstruct the charged hadrons and the photons arising from the neutral pion decays. Both LHC experiments use isolation-based discriminants to remove jet and electron fakes. In addition, both the CDF and the D0 experiments have demonstrated their capability to explicitly reconstruct the neutral pion of the tau decays. Figure 6 shows the

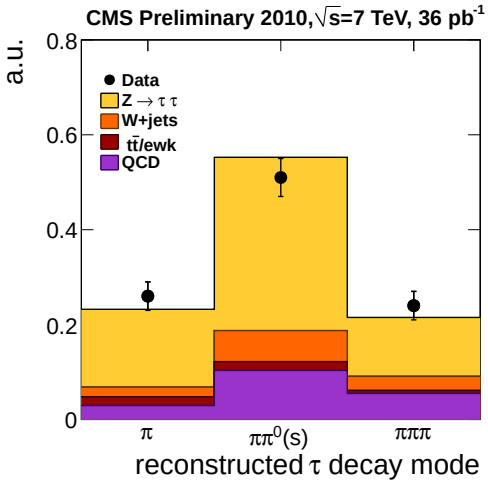

Figure 6: Number of reconstructed tau candidates for the three main decay modes in CMS [14], on 2010 data and for simulated events.

distribution of the reconstructed tau candidates on 2010 collision data in CMS with respect to their decay mode, compared to the predictions for $Z \to \tau\tau$ signal and for the backgrounds.

Finally, multivariate techniques are used to identify tau candidates. Figure 7 show the identification efficiency as a function of the transverse momentum in ATLAS and CMS, for three categories of multivariate criteria. The typical efficiency for the requirements used in top-quark analyses ranges from 40 to 50%.

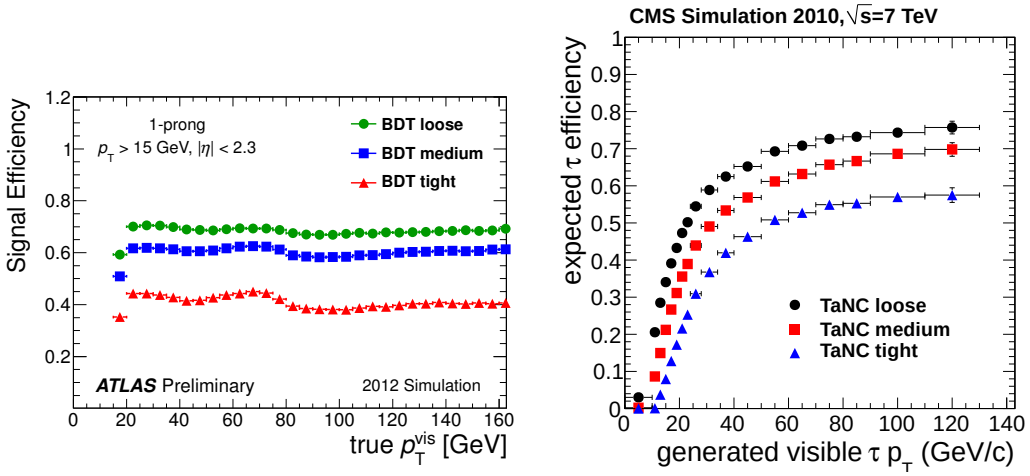

Figure 7: Tau identification efficiency as a function of the transverse momentum in ATLAS [15] (left) and in CMS [14] (right), for three multivariate identification criteria.

4 Energy scale and resolution

Energy scale and resolution are estimated on data in a similar way for electrons, muons and taus. The techniques use "standard candles", such as the Z boson or the J/ψ and Υ meson resonances in the di-lepton invariant mass spectrum, or the distribution of the energy measured

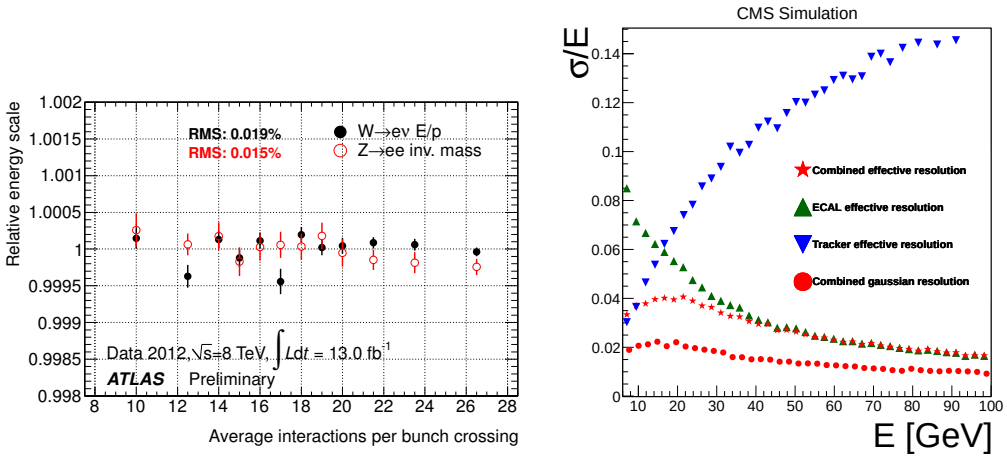

Figure 8: Electron energy scale in ATLAS as a function of the average number of interactions per bunch crossing [10] (left). Electron energy resolution in CMS as a function of the energy [11] (right).

by the calorimeters divided by the momentum measured by the inner tracker of $W \to e\nu$ candidate events.

Figure 8 shows electron energy scale measurements in ATLAS and electron energy resolution measurements as a function of the transverse energy in CMS. Figure 9 shows the di-muon mass resolution in ATLAS as a function of the muon pseudorapidity and the muon transverse momentum resolution as a function of the pseudorapidity in CMS.

The typical uncertainty on the tau energy scale is 3 %, as shown for ATLAS on figure 10. Its effect on the reconstructed tau mass is shown for CMS, on the same figure. Similarly, the energy resolution in these experiments has an uncertainty of a few percent.

5 Impact of lepton systematics on top-quark studies

In the analyses, the impact of the uncertainties on trigger, reconstruction and identification efficiencies on the detector acceptance is most of the time estimated by applying event by event scale-factors on yield and shape predictions based on simulation. These scale-factors are calculated by comparing the efficiencies measured on collision data mainly with "tag-and-probe" techniques to the efficiencies measured with the same techniques on simulated data. Their total uncertainties are propagated to the variables used in each analysis. The impact of these effects is sub-dominant in the case of electrons and muons, especially for top-quark mass measurements where these uncertainties are below 1 %, both at Tevatron or at LHC experiments.

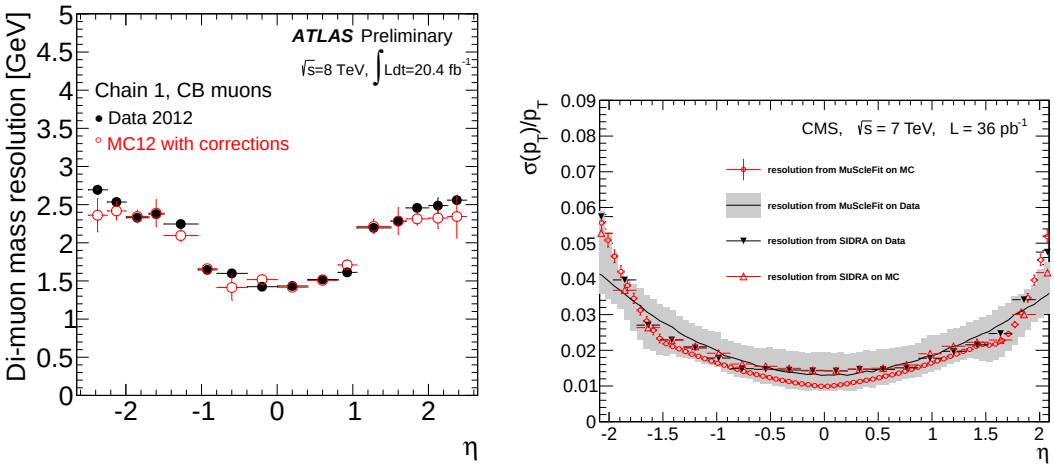

Figure 9: Di-muon mass resolution in ATLAS as a function of the pseudo-rapidity [12] (left). Muon transverse momentum resolution in CMS as a function of the pseudo-rapidity [16] (right).

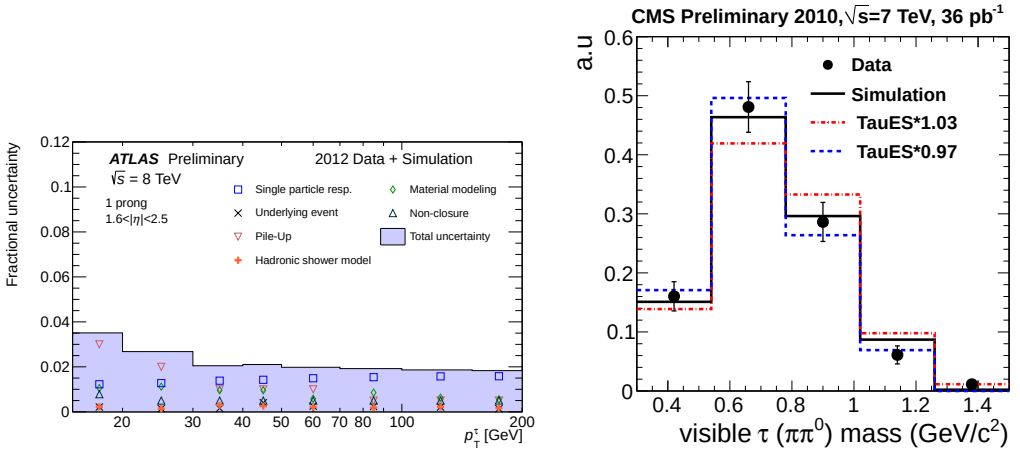

Figure 10: Tau energy scale uncertainty measured on 2012 data and on simulation in ATLAS as a function of transverse momentum, for tau candidates with one track [17] (left). Reconstructed invariant mass of taus decaying into one charged and one neutral pion in CMS, measured on 2010 data and compared with simulation, with nominal or with 3 % shifted tau energy scale [14] (right).

The systematic uncertainty related to the energy scale is measured by varying the energy correction factors by their uncertainties. In a similar way, the uncertainty due to the energy resolution is assessed by varying the resolution by its uncertainty, when smearing the energy on simulation. The propagation of these two effects in top-quark analyses is at most of the order of 1 %.

Aside these detector modelling effects, the measurement of the contribution of reconstructed objects faking prompt leptons gives rise to normalisation and shape uncertainties. Electron and muon fake estimates are described elsewhere. The major source of fake taus are multi-jet and W+jets events. Figure 11 shows the tau fake rates in ATLAS, CMS and CDF as a function of the transverse energy. The typical fake rate value lies between 1 and 3 %, depending on the used identification requirements.

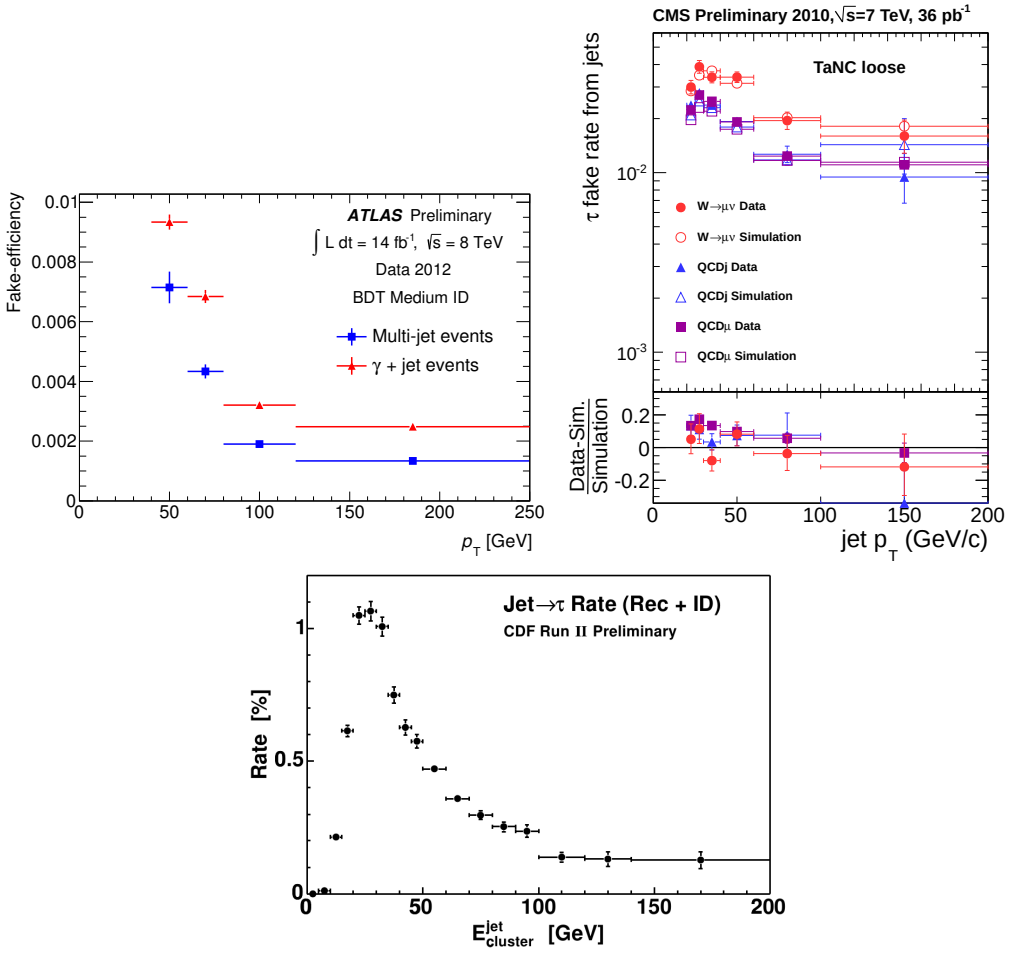

Figure 11: Tau fake efficiency measured on 2012 data in ATLAS as a function of the transverse momentum for a $t\bar{t} \to \tau + jets$ selection [15] (top left). Tau fake efficiency measured on 2010 data in CMS as a function of the transverse momentum for a $Z \to \tau\tau$ selection [14] (top right). Tau fake efficiency measured on simulation in CDF as a function of the transverse energy for jets passing a 50 GeV trigger requirement [18] (bottom).

6 Conclusions

The selection of top-quark events in the semi-leptonic decay modes - where all possible objects are present in the final state - is performed using all subsystems of the general-purpose detectors in the ATLAS, CDF, CMS and D0 experiments. For such events, the trigger relies mainly on single-lepton menus, but multi-object triggering strategies are used in some cases, and may be widely used in the 13 TeV run at the LHC in order to cope with higher rates. Using the full detector granularity allows to reconstruct prompt leptons with high efficiencies, and to reject backgrounds thanks to various identification criteria. The systematic uncertainties related to leptons in top-quark related analyses are rarely greater than a few percent, except when selecting hadronic taus where they can rise up to 8 %, especially in the case of cross-section measurements.

References

[1] D. Acosta *et al.* [CDF Collaboration], Phys. Rev. D **71** (2005) 032001, hep-ex/0412071.

[2] V. M. Abazov *et al.* [D0 Collaboration], Nucl. Instrum. Meth. A **565** (2006) 463, physics/0507191 [physics.ins-det].

[3] G. Aad *et al.* [ATLAS Collaboration], JINST **3**, S08003 (2008).

[4] S. Chatrchyan *et al.* [CMS Collaboration], JINST **3** (2008) S08004.

[5] ATLAS Collaboration, "ATLAS Public Egamma Trigger Plots for Collision Data" https://twiki.cern.ch/twiki/bin/view/AtlasPublic/EgammaTriggerPublicResults

[6] CMS Collaboration, "CMS Trigger Approved Results" https://twiki.cern.ch/twiki/bin/viewauth/CMSPublic/L1TriggerDPGResults

[7] ATLAS Collaboration, "ATLAS Muon Trigger Public Results" https://twiki.cern.ch/twiki/bin/view/AtlasPublic/MuonTriggerPublicResults

[8] ATLAS Collaboration, "ATLAS Tau trigger public results" https://twiki.cern.ch/twiki/bin/view/AtlasPublic/TauTriggerPublicResults

[9] M. Abolins *et al.*, Nucl. Instrum. Meth. A **584** (2008) 75, arXiv:0709.3750 [physics.ins-det].

[10] ATLAS Collaboration, "ATLAS Egamma public results" https://twiki.cern.ch/twiki/bin/view/AtlasPublic/ElectronGammaPublicCollisionResults

[11] CMS Collaboration, "CMS Egamma Results" https://twiki.cern.ch/twiki/bin/view/CMSPublic/PhysicsResultsEGM

[12] ATLAS Collaboration, ATLAS-CONF-2013-088.

[13] CMS Collaboration, "CMS Muon Results" https://twiki.cern.ch/twiki/bin/view/CMSPublic/PhysicsResultsMUO

[14] CMS Collaboration, CMS-PAS-TAU-11-001.

[15] ATLAS Collaboration, ATLAS-CONF-2013-064.

[16] S. Chatrchyan *et al.* [CMS Collaboration], JINST **7** (2012) P10002, arXiv:1206.4071 [physics.ins-det].

[17] ATLAS Collaboration, ATLAS-CONF-2013-044.

[18] S. Levy on behalf of the CDF and D0 Collaborations, Springer Proc. Phys. **108** (2006) 102.